The American Journal of Pathology, Vol. 169, No. 2, August 2006

DOI: 10.2353/ajpath.2006.050981

Musculoskeletal Pathology

Functional Knockout of the Matrilin-3 Gene Causes Premature Chondrocyte Maturation to Hypertrophy and Increases Bone Mineral Density and Osteoarthritis

Louise van der Weyden,* Lei Wei,† Junming Luo,† Xu Yang,† David E. Birk,‡ David J. Adams,* Allan Bradley,* and Qian Chen†

From the Mouse Genomics Lab, Wellcome Trust Sanger Institute, Wellcome Trust Genome Campus, Cambridge, United Kingdom; the Department of Orthopaedics,† Brown Medical School/Rhode Island Hospital, Providence, Rhode Island; and the Department of Pathology, Anatomy, and Cell Biology,‡ Thomas Jefferson University, Philadelphia, Pennsylvania*

Mutations in the gene encoding matrilin-3 (*MATN3*), a noncollagenous extracellular matrix protein, have been reported in a variety of skeletal diseases, including multiple epiphyseal dysplasia, which is characterized by irregular ossification of the epiphyses and early-onset osteoarthritis, spondylo-epimetaphyseal dysplasia, and idiopathic hand osteoarthritis. To assess the role of matrilin-3 in the pathogenesis of these diseases, we generated *Matn3* functional knockout mice using embryonic stem cell technology. In the embryonic growth plate of the developing long bones, *Matn3* null chondrocytes prematurely became prehypertrophic and hypertrophic, forming an expanded zone of hypertrophy. This expansion was attenuated during the perinatal period, and *Matn3* homozygous null mice were viable and showed no gross skeletal malformations at birth. However, by 18 weeks of age, *Matn3* null mice had a significantly higher total body bone mineral density than *Matn1* null mice or wild-type littermates. Aged *Matn3* null mice were much more predisposed to develop severe osteoarthritis than their wild-type littermates. Here, we show that matrilin-3 plays a role in modulating chondrocyte differentiation during embryonic development, in controlling bone mineral density in adulthood, and in preventing osteoarthritis during aging. The lack of *Matn3* does not lead to postnatal chondrodysplasia but accounts for higher incidence of osteoarthritis. *(Am J Pathol 2006, 169:515–527; DOI: 10.2353/ajpath.2006.050981)*

The matrilins are a four-member family of oligomeric extracellular matrix (ECM) proteins containing common structural motifs including von Willebrand factor A (vWFA) domains, epidermal growth factor (EGF)-like domains, and coiled-coil domains (reviewed in Ref. [1]). Matrilin-1 (also known as cartilage matrix protein) and matrilin-3 are abundant in cartilage,[2–4] whereas matrilin-2 and matrilin-4 show a broader tissue distribution.[1,3,5,6] All matrilins form homo-oligomers through assembly of C-terminal coiled-coil structures, and matrilin-1 and matrilin-3 can form hetero-oligomers.[4,7,8] The matrilins are thought to play a role in the ECM by acting as bridges to connect matrix components in the cartilage to form macromolecular networks: matrilin-1 interacts with type II collagen[9] and aggrecan,[10,11] and matrilins-1, -3, and -4 have been shown to associate with collagen type VI and connect these networks to aggrecan and collagen type II.[12]

Matrilin-3 is the least complex member of the matrilin family, consisting of only one vWFA domain, four EGF-like domains, and a C-terminal coiled-coil domain.[3] The vWFA domain is found in various collagenous and noncollagenous extracellular matrix proteins[13] and is composed of a central β-sheet core flanked by α-helices. In humans, nine missense mutations in the matrilin-3 gene (*MATN3*) that affect the vWFA domain (typically the β-sheets) have been found in patients with multiple epiphyseal dysplasia (MED), characterized by delayed and irregular ossification of the epiphyses and early-onset osteoarthritis.[13–17] Mutations in *MATN3* have also been reported in other osteochondrodysplasias, including bilateral hereditary microepiphyseal dysplasia, a MED-like disorder characterized by small epiphyses in

Supported by a CJ Martin/RG Menzies fellowship (to L.v.d.W.) and a CJ Martin fellowship (D.J.A.) from the National Health and Medical Research Council of Australia, by the National Institutes of Health (Q.C., L.W., and D.E.B.), and by the Arthritis Foundation (Q.C.).

Accepted for publication April 27, 2006.

Address reprint requests to Prof. Qian Chen, Suite 402, 1 Hoppin St., Providence, RI 02903. E-mail: qian_chen@brown.edu.

the hip and knee joints,[15] spondylo-epimetaphyseal dysplasia, which includes a number of conditions associated with vertebral, epiphyseal, and metaphyseal anomalies,[18] and idiopathic hand osteoarthritis.[19] Matrilin-3 has also been reported to be up-regulated in cartilage from osteoarthritis patients with a strong correlation between enhanced matrilin-3 gene and protein expression and the extent of tissue damage.[20] These findings suggest that tight regulation of matrilin-3 expression is essential for maintenance of the cartilage ECM microenvironment. However, it is not known how defective matrilin-3 leads to a variety of skeletal diseases including both chondrodysplasia during development and osteoarthritis in adulthood.

In the mouse, matrilin-3 is expressed exclusively in the developing cartilage of the skeletal system, with expression first being detected at day 12.5 and remaining unchanged from embryonic day (E) 15.5 until birth.[21] In newborn mice, matrilin-3 is widely expressed in the cartilage of the developing bones of the eye, nasal cavity, ribs, long bones, sternum, and trachea, but its expression is more restricted by 6 weeks of age.[4,22] Although it has been shown that matrilin-1 and -3 can form heterooligomers and are often colocalized in tissue, clear differences in their spatial distribution have been shown by double immunolabeling.[22] In addition, although matrilin-1 expression continues in tissues that remain cartilaginous throughout life (such as in costal cartilage and in the nasal septum), matrilin-3 expression ceases after birth in these tissues.[22]

Matrilin-1 has been inactivated by gene targeting in the mouse by two different groups. In one case, no abnormalities were reported,[23] whereas the other group reported alterations in cartilage collagen fibril organization and fibrillogenesis.[24] More recently, matrilin-3 has been inactivated by targeted disruption in the mouse and was found to be dispensable for normal skeletal growth and development in peri- or postnatal stages, with histological and ultrastructural analyses revealing endochondral bone formation indistinguishable from that of wild-type animals.[25] Given that matrilin-3 has been implicated in the pathogenesis of both chondrodysplasia and osteoarthritis, in the present study, we have generated a new allele of matrilin-3 and used these homozygous matrilin-3 functional knockout mice to examine the role of matrilin-3 in cartilage during embryonic development and adulthood. We show for the first time its role in the development of osteoarthritis during aging.

Materials and Methods

Generation of Matrilin 3-Deficient Mice

A 500-bp *Matn3* exon 2 cDNA probe was used to screen the RPCI-23 BAC filter library and isolate clone RP23-447f3. Using the BAC clone as a template, polymerase chain reaction (PCR) was performed using Platinum PCR Supermix High Fidelity (Invitrogen, Carlsbad, CA) for 18 amplification cycles to generate the homology arms of the targeting vector. The 5′ homology arm consisted of a 3.9-kb *Eco*RV-flanked product (spanning from the 5′-untranslated region to the first few amino acids of exon 2) with a stop codon incorporated into the 3′ end. The 3′ homology arm consisted of a 5-kb *Not*I-flanked product (spanning from the last few amino acids of exon 2 to intron 3) and introduced an *Sst*I restriction site at the 3′ end. The PCR products were cloned into pGEM-T Easy (Promega, Madison, WI) and sequenced to ensure no mutations had been introduced during amplification before being cloned into a phosphoglycerate kinase-neomycin cassette-containing vector.

Ten micrograms of the *Sal*I-linearized *Matn3* targeting vector (pM29) was electroporated into AB2.2 embryonic stem (ES) cells (from mouse strain 129S5/SvEvBrd).[26] The ES cells were cultured on a lethally irradiated SNL76/7 feeder layer[27] and picked into 96-well plates after 7 days of drug selection in G418 (180 μg/ml). To check for homologous recombination, genomic DNA was analyzed by Southern blotting using both 520-bp 5′ external probe pO1 (forward, 5′-GCATCCCATTCACGATGCTAGAATTTGTGAGGC-3′; reverse, 5′-ATGGGCTTGACGACCTGCCGGGGTCTGTGAGC-3′) on *Spe*I-digested DNA to identify a 12-kb wild-type allele and a 7.6-kb targeted allele and a 554-bp 3′ external probe pM4 (forward, 5′-AGTCTAGCAAAGCAAGACCTTTATTTGCATTAGGCATAAA-3′; reverse, 5′-AGGAGTGGGCACAGGAAAGGGAACTGATGGAATTTCTGGT-3′) on *Sst*I-digested DNA to identify a 9-kb wild-type allele and a 6-kb targeted allele. Correctly targeted ES cell clones termed *Matn3*^{Brdtm1} (*Matn3*$^{m1/+}$) were injected into C57BL/6J blastocysts for germline transmission as described previously,[26] and germline transmission of the targeted (mutant) allele was demonstrated by Southern blot analysis of tail DNA using both probes. Mice were maintained on a mixed 129/C57 background and housed in accordance with Sanger Institute home office regulations (United Kingdom). The matrilin-1 null (*Matn1*$^{-/-}$) mice were imported from Paul Goetinck (Harvard Medical School, Boston, MA) and have been previously described.[24]

RNA Isolation, Reverse Transcription (RT)-PCR, and Real-Time Quantitative RT-PCR

Total RNA was extracted from the hind limb of *Matn3* wild-type and null (*m1/m1*) embryos at day E18.5 using the RNAqueous kit (Ambion, Austin, TX) according to the manufacturer's instructions. For RT-PCR, 1.5 μg of RNA was reverse-transcribed using RETROscript (Ambion) according to the manufacturer's instructions, and the resulting cDNA was used in PCR analysis of the expression of *matrilin-3* using primers spanning exon 2 (GenBank accession no. NM_010770; forward, 5′-AGGTGTTTGCAAGAGCAGGCCTTTGGACTT-3′; reverse, 5′-CAAAAGGTTTCCTGGAATCTAGCAGAAAGC-3′; 570-bp product) and exons 1 to 3 (forward, 5′-ATGTTGCTCTCAGCCCCCTTACGCC-3′; reverse, 5′-GTGCCAAGCATGCACTGATCCAGA-3′; 800-bp product); *matrilin-1* using primers spanning exons 2 to 3 (GenBank accession no. NM_010769; forward, 5′-ACGGACCTGGTGTTTGTTGT-

3′; reverse, 5′-AGAAGGCCTCTTGGAACT-3′; 544-bp product); and *β-actin* using primers spanning exons 2 to 3 (GenBank accession no. NM_007393; forward, 5′-ACCAACTGGGACGATATGGAGAAGA-3′; reverse, 5′-TACGACCAGAGGCATACAGGGACAA-3; 215-bp product). The cDNA was amplified in 50-μl reactions using 45 μl of Platinum PCR Supermix (Invitrogen) and 100 ng of each primer pair with the following PCR cycle profile: 1 cycle at 94°C for 2 minutes followed by 30 cycles at 94°C for 30 seconds, 65°C for 1 minute, and 72°C for 30 seconds with a final cycle of 72°C for 10 minutes. All PCR products were cloned into pGEM-T Easy (Promega) and sequenced to confirm their identity.

For real-time quantitative RT-PCR, 1 μg of total RNA was used for each reverse transcriptase reaction in a reaction buffer containing 1 μl of oligo(dT) and 1 μl of 10 mmol/L dNTP Mix (Ambion). Real-time quantitative PCR amplification was performed using QuantiTect SYBR Green PCR kit (Qiagen, Valencia, CA) with DNA Engine Opticon 2 Continuous Fluorescence Detection System (MJ Research, Waltham, MA). Primers used in amplification of target genes' mRNA are as follows: *Matrilin-1* (forward, 5′-CCCCCGACATCAGCAAGGTT-3′; reverse, 5′-CGCAGCGTAGCCTTGTCCAC-3′), *Matrilin-2* (forward, 5′-TGCCTCTGAGCCCATTGACAAG-3′; reverse, 5′-TATGTTGCACTGTTGGCTGGT-3′), *Matrilin-4* (forward, 5′CCGCGAGGACATGGAACGA 3′; reverse, 5′TGCGAAGAGAGCCCACGTCA 3′), *Ihh* (forward, 5′-CCACTTCCGGGCCACATTTG-3′; reverse, 5′-GGCCACCACATCCTCCACCA-3′), *Type X collagen* (forward, 5′-CCAGGTGTCCCAGGATTCCC-3′; reverse, 5′-CAAGCGGCATCCCAGAAAGC-3′), *VEGF* (forward, 5′-CCTGGTAATGGCCCCTCCTC-3′; reverse, 5′-CCCCATTGCTCTGTGCCTTG-3′), and *18S RNA* (forward, 5′-CGGCTACCACATCCAAGGAA-3′; reverse, 5′-GCTGGAATTACCGCGGCT-3′). All target gene mRNA levels were normalized to housekeeping gene 18S RNA levels. Calculation of mRNA values was performed as previously described.[8] The 18S RNA was amplified at the same time and used as an internal control. The cycle threshold (Ct) values for 18S RNA and that of samples were measured and calculated by computer software (PE ABI, Foster City, CA). Relative transcript levels were calculated as $x = 2^{-\Delta\Delta Ct}$, in which $\Delta\Delta Ct = \Delta E - \Delta C$, and $\Delta E = Ct_{exp} - Ct_{18s}$; $\Delta C = Ct_{ctl} - Ct_{18s}$.

Data were presented as mean ± SEM for six animal samples and analyzed using two-way analysis of variance. The level of each gene in wild-type limb tissues was designated as 1. Statistical significance was taken at *P* values of less than 0.05 ($P < 0.05$).

Skeletal Staining and Radiographical Analysis

Skeletons of *Matn3* null (*m1/m1*) and wild-type (+/+) embryos (E17.5) and newborn (P1) mice were prepared and stained with alcian blue and alizarin red as described previously.[28] For radiographical analysis, male and female *Matn3* null and wild-type mice were euthanized at 7, 18, and 52 weeks of age and images taken with a PIXImus II Bone Densitometer (X-ray tube, 80/35 kVp at 0.5 mA; GE Medical Systems, Bedford, United Kingdom). The PIXImus software package automatically analyzes the resulting images to calculate bone area, bone mineral content, bone mineral density (BMD; bone mineral content/bone area), lean tissue, fat tissue, and percentage of fat. For whole-body measurements, the skull was excluded and for knee joint measurements, a standard "inclusion region of interest" (40 × 40 pixels) was used to gate the knee joint. For Faxitron analysis, knee joints from *Matn3* null and wild-type mice at 1 year of age were dissected free of surrounding tissues and imaged with a Faxitron X-ray MX-20 (Faxitron X-ray Corporation, Wheeling, IL).

Histology

Hind limbs dissected from *Matn3* null (*m1/m1*) and wild-type (+/+) embryos at ages E12.5 to E18.5 and newborn mice (P1) were fixed overnight in 4% paraformaldehyde in phosphate-buffered saline (pH 7.4), dehydrated in ethanol, cleared in xylene, and embedded in paraffin, and 6-μm sections were cut. Samples taken after birth were decalcified in 10% ethylenediamine tetraacetic acid-phosphate-buffered saline (PBS) for up to 2 weeks before being processed. For histology, sections were stained with hematoxylin and eosin (H&E) according to standard histochemical protocols. For Safranin-O/Fast Green staining, 5-μm paraffin-embedded sections of tibia from mice were counterstained with hematoxylin before being stained with 0.02% aqueous Fast Green for 4 minutes (followed by three dips in 1% acetic acid) and then 0.1% Safranin-O for 6 minutes. The slides were then dehydrated and mounted with crystal mount medium. At least five animals from each stage were collected for histological analysis. The hypertrophic zone was defined by visual inspection of enlarging cell size in the zone on the histology slide and by expression of type X collagen mRNA through *in situ* hybridization analysis. Comparison of healthy (grade 0) and osteoarthritis (OA) cartilage morphological changes was determined by modified Wilhelmi OA scoring system[29] with the single worst affected score of H&E paraffin slides through the entire knee joint. At least two blinded observers scored the cartilage sections. Significance of scores between *Matn3* null (*m1/m1*) and wild-type (+/+) mice was determined by χ^2 statistics.

Immunohistochemistry

For immunohistochemistry, sections were digested with bovine testicular hyaluronidase (4000 U/ml in PBS; Sigma, St. Louis, MO) for 30 minutes at 37°C. After washing in PBS, the sections were incubated with 5% normal goat serum for 30 minutes at room temperature before being incubated for 1 hour at room temperature with either polyclonal anti-collagen type II antibody (Chemicon Europe Ltd., Hampshire, United Kingdom), anti-matrilin-1 monoclonal antibody 1H1,[30] or anti-matrilin-2 monoclonal antibody (to generate a polyclonal antibody against matrilin-2, a peptide encoding 20 amino acids

[SRSTQKLFHSTKSSGNPLEE] from the unique domain of mouse matrilin-2 was synthesized and the antibody was raised by immunizing rabbits with the synthetic peptide followed by affinity purification). Affinity-purified fluorescein-conjugated or phycoerythrin-conjugated secondary antibodies (Jackson ImmunoResearch, West Grove, PA) were then applied at 1:100 for 1 hour at room temperature.

Distribution of proliferating cell nuclear antigen (PCNA) antigen in growth plate was examined by immunohistochemistry with a Histostain SP kit (Zymed, San Francisco, CA) using anti-PCNA monoclonal antibody (sc-56; Santa Cruz Biotechnology, Santa Cruz, CA) as primary antibody, as described in *http://www.ihcworld.com/_protocols/antibody_protocols/pcna_santa_cruz.htm*.

After hyaluronidase treatment, deparaffinized sections were incubated in 0.2% Triton X-100/PBS for 5 minutes at room temperature. Slides were washed with PBS and treated with peroxidase-quenching solution to eliminate endogenous peroxidase activity. After blocking with a blocking solution for 10 minutes at room temperature, sections were then incubated with primary antibodies (1:100) for 1 hour at 37°C followed by incubation overnight at 4°C. After washing, the sections were incubated at room temperature with biotinylated secondary antibodies for 10 minutes, with a streptavidin-peroxidase conjugate for 10 minutes, and with a solution containing diamino-benzidine (chromogen) and 0.03% hydrogen peroxide for 5 minutes. Sections were counterstained with hematoxylin, dehydrated, and mounted. Photography was performed with a Nikon microscope. The length ratio of the hypertrophic zone was calculated as the length of the hypertrophic zone over the total length of proximal tibial growth plate. PCNA-positive cellular profiles were calculated as the percentage of total counted cellular profiles in the different zones of proximal tibial growth plates. A total of 16 sections from four animals were used to perform PCNA study. Statistical analysis was performed using Student's *t*-test after consultation with a statistician to ensure the proper sample sizes. Data were expressed as mean ± SD.

In Situ *Hybridization*

In situ hybridizations were performed as previously described.[31] Sense and antisense ^{35}S-labeled RNAs were synthesized from the linearized plasmids using the riboprobe systems kit (Promega) and [^{35}S]UTP (Amersham, Piscataway, NJ). Sense RNA was used as control. The following cDNA plasmids were used: aggrecan, collagen type X, and Sox 9 cDNA plasmids were provided by Prof. Kathy Cheah (University of Hong Kong, Hong Kong), the Indian hedgehog cDNA plasmid was provided by Dr. Andrew McMahon (Harvard University), and the parathyroid hormone-related peptide cDNA plasmid was provided by Dr. Trevor Williams (University of Colorado Health Sciences Center, Denver, CO).

Transmission Electron Microscopy

Hind limbs dissected from *Matn3* null (*m1/m1*) and wild-type (+/+) embryos (E17.5) and newborn (P1) mice were fixed in 4% paraformaldehyde/2.5% glutaraldehyde/0.1 mol/L sodium cacodylate, pH 7.4, with 8 mmol/L $CaCl_2$ for 15 minutes at room temperature, during which time the skin and muscle was dissected away. After this time, the tissue was incubated at 4°C for 40 minutes before being processed as described previously.[32] Tibia and femur from six animals from each stage were analyzed. Sections were viewed in an electron microscope (CM10; Philips Electronic Instruments, Inc., Mahwah, NJ).

Results

Generation of Matrilin-3 Null Mice

Like the human matrilin-3 gene (*MATN3*), the mouse homolog *Matn3* consists of eight exons: exon 1 encodes a signal peptide and a positively charged domain; exon 2, the vWFA domain; exons 3 to 6, the four EGF-like domains; and exons 7 and 8, a coiled-coil domain (Figure 1A). Because the vWFA domain is the site of all nine *MATN3* mutations in MED patients and vWFA domains are thought to mediate interactions with other proteins, we chose to ablate exon 2 of *Matn3* by homologous recombination in ES cells and replace it with a neomycin resistance cassette and an in-frame stop codon (Figure 1A). AB2.2 ES cells were electroporated with the nonisogenic targeting vector, pM29 (Figure 1A). Of the 1000 G418-resistant ES cell clones that were picked, two correctly targeted clones were identified by Southern blot analysis of *Spe*I- and *Sst*I-digested genomic DNA using a 5′ (pO1) and 3′ (pM1) external probe, respectively (data not shown). ES cells from the two targeted clones were used to generate chimaeras, which transmitted the targeted allele *Matn3^{Brdm1}* (*m1*) to their progeny. Heterozygous mice were intercrossed to produce wild-type, heterozygous, and homozygous offspring (Figure 1B) in normal Mendelian ratios. To confirm that the mutant allele was a null, RT-PCR was performed on RNA extracted from the hind limbs of embryonic day 17.5 wild-type and homozygous (*m1/m1*) mutant mice. Using primers designed against exon 2, the expected 570-bp product was produced from RNA from wild-type but not *m1/m1* mice (Figure 1C). Using primers designed against exons 1 to 3, RNA from wild-type mice produced the expected 800-bp product, whereas RNA from *m1/m1* mice produced a 225-bp product (Figure 1C), which when sequenced showed a splicing of exon 1 with exon 3 (Figure 1C, box). The skipping of exon 2 in the *m1* allele results in a reading frame shift that would be predicted to result in a nonsense protein, containing the signal peptide region but not any of the major domains of matrilin-3. Therefore, it is not expected to serve a dominant-negative function, and we conclude that the *Matn3^{Brdm1}* allele is a null.

Matrilin-3 Null Mice Show No Gross Skeletal Abnormalities at Birth

Matn3 null mice were healthy at birth. Both males and females were fertile and had a normal lifespan. Because matrilin-3 is expressed by chondrocytes and osteoblasts during endochondral bone formation,[4] we analyzed the

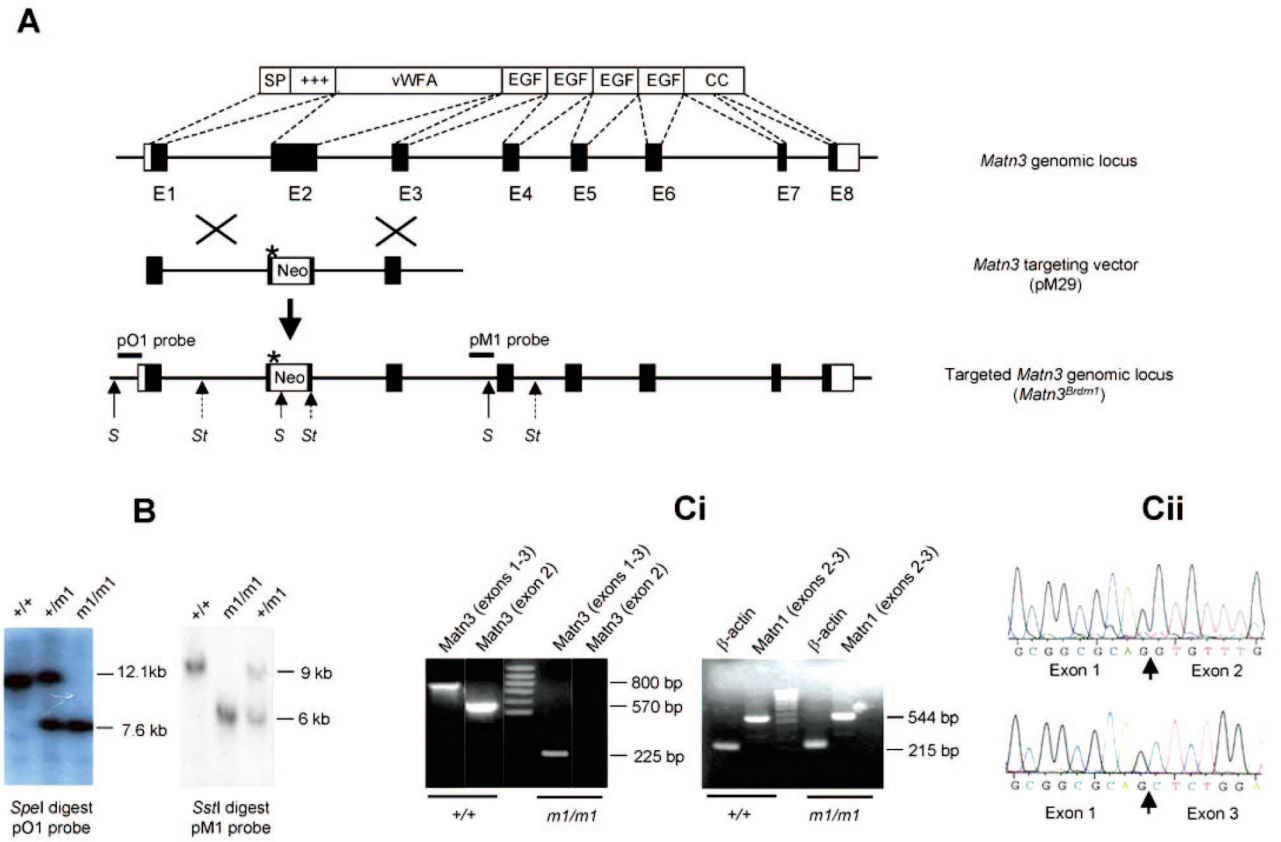

Figure 1. Targeting strategy and genotypic analysis of matrilin-3 null (*Matn3*^{Brdm1}) mice. **A:** Schematic of the *Matn3* gene and corresponding encoded protein showing the wild-type genomic locus, targeting vector (pM29), and targeted allele (*Matn3*^{Brdm1}). The neomycin resistance cassette (Neo) replaces exon 2, which encodes the vWFA domain. The **asterisk** indicates an in-frame stop codon that was introduced into the 3′end of the 5′ arm of the targeting vector. The relative location of the 5′ and 3′ probes and restriction enzyme sites (S, *Spe*I; St, *Sst*I) that were used in Southern blot analysis are shown on the targeted allele. **B:** Southern blot analysis of wild-type (+/+), heterozygous (+/*m1*), and homozygous (*m1/m1*) *Matn3* mouse tail genomic DNA from that was digested with either *Spe*I and hybridized with the pO1 probe or *Sst*I and hybridized with the pM1 probe. **Ci:** RT-PCR analysis of RNA isolated from wild-type (+/+) and *Matn3* null (*m1/m1*) limbs. Using primers designed against exons 1 to 3, RNA from wild-type mice produced the expected 800-bp product, whereas RNA from *m1/m1* mice produced a 225-bp product due to the deletion of exon 2 and splicing of exon 1 with exon 3, which causes a reading frame shift predicted to result in a nonsense protein (**Cii**).

gross skeletal morphology of embryonic and adult *Matn3* null mice. Staining of E17.5 and newborn (P1) *Matn3* null mice with alcian blue (for cartilage) and alizarin red (for bone) showed no obvious differences from wild-type littermates (Figure 2A). Radiographical analysis of 7- and 18-week-old *Matn3* null mice showed no gross skeletal malformations (Figure 2B). Thus the lack of matrilin-3 does not appear to grossly affect normal skeletal patterning and growth.

Because *Matn1* null mice have been reported to show alterations in type II collagen fibrillogenesis and fibril organization,[24] we examined extracellular matrix organization in cartilage of *Matn3* null mice. Ultrastructural analysis of extracellular matrix in proximal epiphyseal growth plates from E17.5 and newborn (P1) *Matn3* null mice showed a normal network of collagen fibrils with no appreciable difference in collagen fibril diameters (Figure 2C).

Expression and Distribution of the Other Matrilins in Matrilin-3 Null Mice

To determine whether the absence of an overt *Matn3* null phenotype was due to compensation by other members of the matrilin family, we analyzed expression of other matrilins. Real-time quantitative RT-PCR indicated that there were no significant differences in the levels of mRNAs encoding matrilin-1, -2, and -4 in newborn *Matn3* null mice compared with wild-type littermates (Figure 3A). Thus there is no evidence of a compensatory up-regulation of other members of the matrilin family in *Matn3* null mice. Immunostaining of tibiae showed normal expression patterns of matrilin-1 and -2 in the proximal epiphyseal growth plate of *Matn3* null mice, with matrilin-1 present in the proliferating zone and the prehypertrophic zone and matrilin-2 present in the hypertrophic zone (Figure 3B). However, the hypertrophic zone in a *Matn3* null proximal growth plate was expanded in comparison with the wild-type at E16.5 and E17.5 (Figure 3B). Histological analysis indicated that the length of the hypertrophic zone was increased by 47% in *Matn3* null mice compared with wild-type littermates at E16.5 (Figure 3C). The expansion of the hypertrophic zone in *Matn3* null proximal tibial growth plates was attenuated during perinatal development, and no difference of the length of the hypertrophic zone was observed between wild-type and *Matn3* null growth plates in newborn mice.

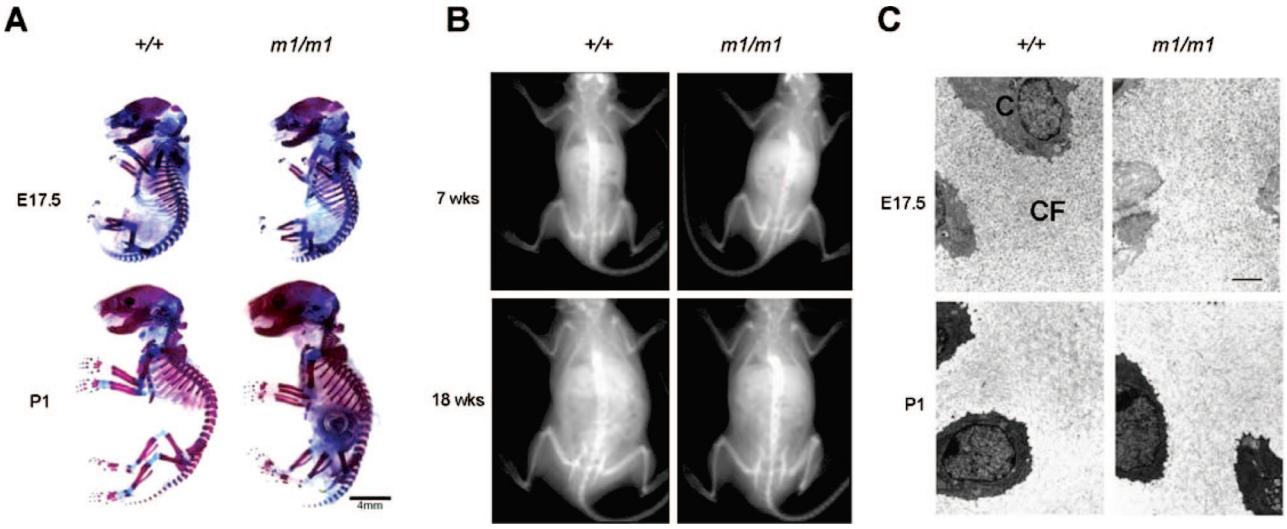

Figure 2. Analysis of skeletal development in *Matn3* null mice. **A:** Skeletal preparations of E17.5 and newborn (P2) wild-type (+/+) and *Matn3* null (*m1/m1*) littermates. Alcian blue stains nonmineralized cartilage, and alizarin red stains mineralized cartilage and bone. **B:** Radiographical analysis of 7- and 18-week-old wild-type and *Matn3* null littermates. Image area represents 80 × 65 mm. **C:** Ultrastructural analysis of the extracellular matrix in tibial proximal epiphyseal growth plates from E17.5 and newborn (P1) wild-type and *Matn3* null littermates was performed by electron microscopy. C, chondrocytes; CF, collagen fibrils. Scale bar = 5 μm.

Matrilin-3 Null Chondrocytes Prematurely Become Prehypertrophic during Embryonic Development

To determine the mechanistic basis of the expansion of the hypertrophic zone in *Matn3* null embryonic growth plates, we analyzed *Matn3* null proximal tibial growth plates in more detail. Immunohistochemical analysis of PCNA staining, a marker of cell proliferation, showed that the percentage of the proliferating cellular profiles was significantly decreased in the columnar regions of *Matn3* null embryonic growth plate in comparison with the wild-type (Figure 4C). This indicated that *Matn3* null chondrocytes exit cell cycle precociously.

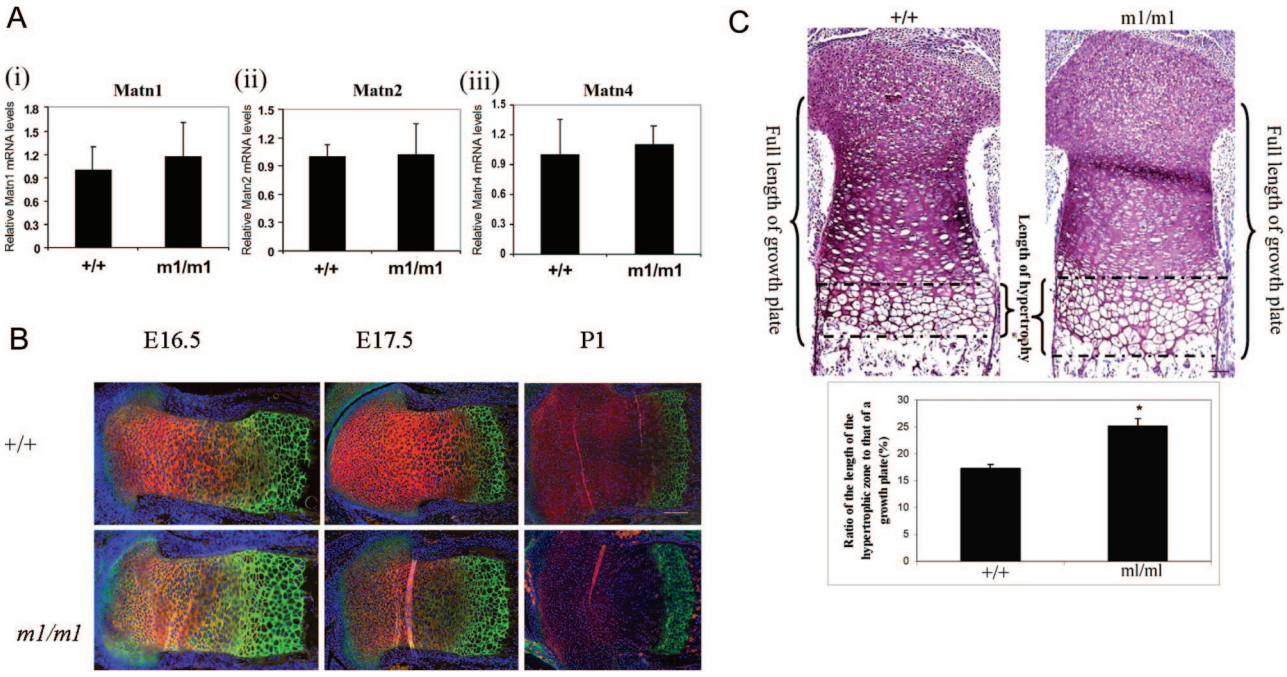

Figure 3. Expression and distribution of other members of the matrilin family in *Matn3* null mice. **A:** Real-time quantitative RT-PCR analysis of RNA isolated from E18.5 wild-type (+/+) and *Matn3* null (*m1/m1*) limbs shows there is no compensatory up-regulation of the *Matn1*, *Matn2*, or *Matn4* isoforms. **B:** Immunohistochemical staining of proximal tibial epiphyses from E16.5, E17.5, and newborn (P1) littermates shows normal expression patterns of matrilin-1 (red) and matrilin-2 (green) in the epiphyseal growth plate. Scale bar = 200 μm. **C:** Measurement of the hypertrophic zone profile of proximal tibial epiphyses from embryonic day 17.5 littermates shows a significant increase of the ratio (%) of the hypertrophic zone length to the overall length of the growth plate. As indicated, the length of the growth plate starts from the most proximal part of the proliferating cell zone and ends at the most distal part of the hypertrophic zone. Sections were stained with Safranin-O/Fast Green. Scale bar = 200 μm.

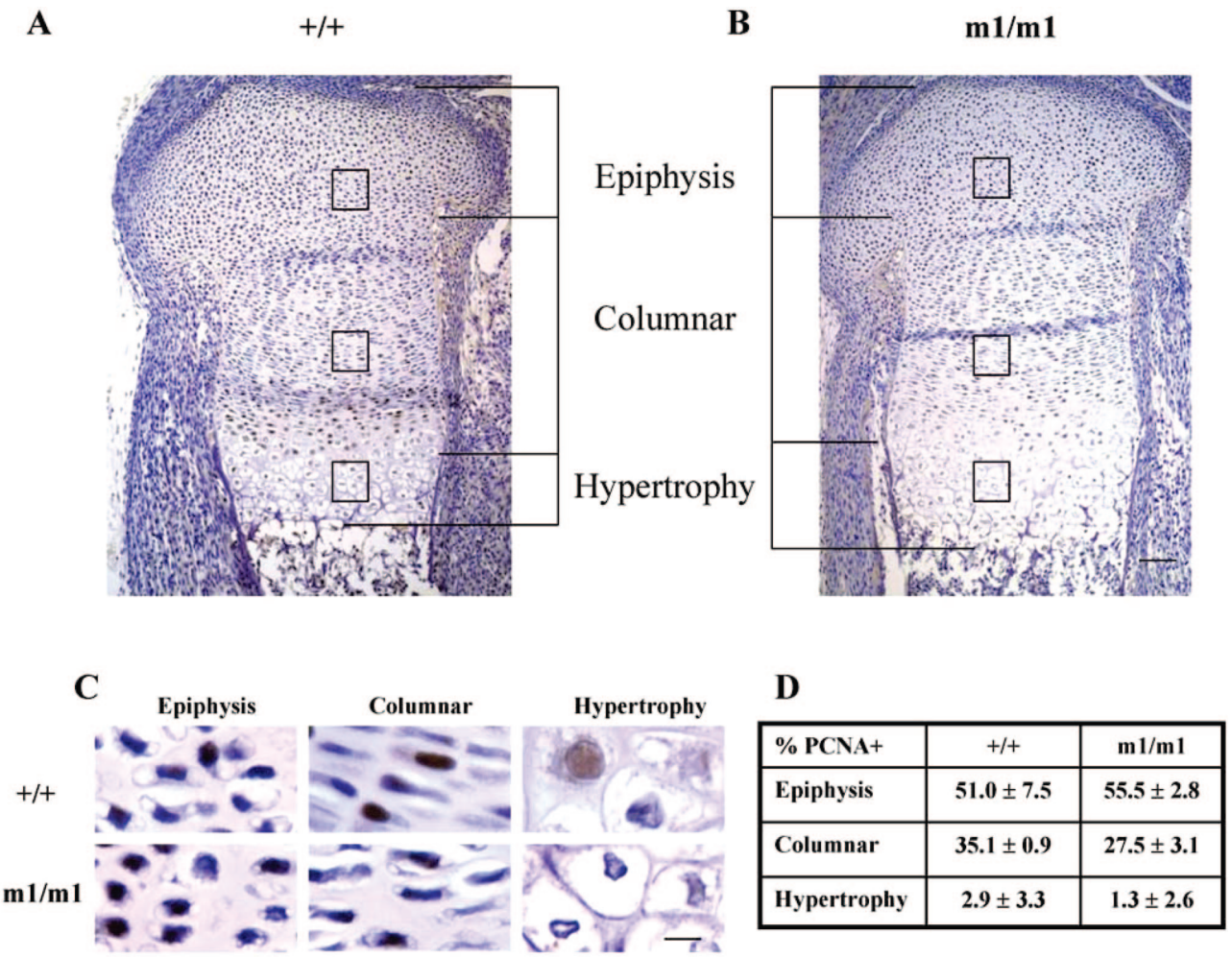

% PCNA+	+/+	m1/m1
Epiphysis	51.0 ± 7.5	55.5 ± 2.8
Columnar	35.1 ± 0.9	27.5 ± 3.1
Hypertrophy	2.9 ± 3.3	1.3 ± 2.6

Figure 4. Analysis of the expanded hypertrophic zone in the embryonic growth plate of *Matn3* null mice. **A** and **B:** Analysis of H&E-stained sections of E16.5 proximal tibial epiphyseal growth plates shows that the length of the hypertrophic zone was increased in *Matn3* null (*m1/m1*) mice compared with wild-type (+/+) littermates. Scale bar = 200 μm. **C** and **D:** Immunohistochemical analysis of cell proliferation by counting cellular profiles positive for anti-PCNA antibody staining showed the percentage of the proliferating cellular profiles was significantly decreased in the columnar regions of *Matn3* null embryonic E16.5 growth plate in comparison with the wild type. Scale bar = 50 μm.

We investigated markers for chondrocyte differentiation in the proximal tibial growth plate of *Matn3* null mice (Figure 5A). *In situ* hybridization of the tibia from E16.5 *Matn3* null mice showed intense aggrecan mRNA signals in the prehypertrophic zone. The expression area of collagen type X mRNA, a marker of the hypertrophic chondrocytes, was expanded in *Matn3* null growth plates. These data indicated that *Matn3* null chondrocytes undergo premature differentiation to the hypertrophic stage. *In situ* hybridization was performed using probes for genes involved in signaling pathways important for the regulation of bone growth. The expression domain of Indian hedgehog (Ihh), which is expressed by prehypertrophic chondrocytes, was expanded in the *Matn3* null growth plate in comparison with the wild-type. *Sox9* mRNA signals were decreased in *Matn3* null mice, and the mRNA signals of the parathyroid hormone-related peptide (*PTHrP*) were diminished in the perichondrium regions next to the prehypertrophic and hypertrophic zones in *Matn3* null mice (Figure 5A).

To further determine which stage of chondrocyte differentiation was affected by *Matn3*, we performed real-time PCR to quantify the mRNA levels of *Ihh*, which is synthesized by prehypertrophic chondrocytes; *Col X*, which is synthesized by hypertrophic chondrocytes; and vascular endothelial growth factor (*Vegf*), which is synthesized by late hypertrophic chondrocytes (Figure 5B). Levels of *Ihh* and *Col X* were significantly increased in *Matn3* null chondrocytes, which is consistent with the *in situ* hybridization analysis. However, the level of VEGF was not affected. Taken together, these data suggest that expanded hypertrophic zone seen in *Matn3* null mice is due to accelerated differentiation (prehypertrophy and hypertrophy) rather than delayed matrix resorption.

Elevated Bone Mass Density in Adult Matrilin-3 Null Mice

Although the *Matn3* null mice showed no obvious gross abnormalities in bone structure, we wanted to determine

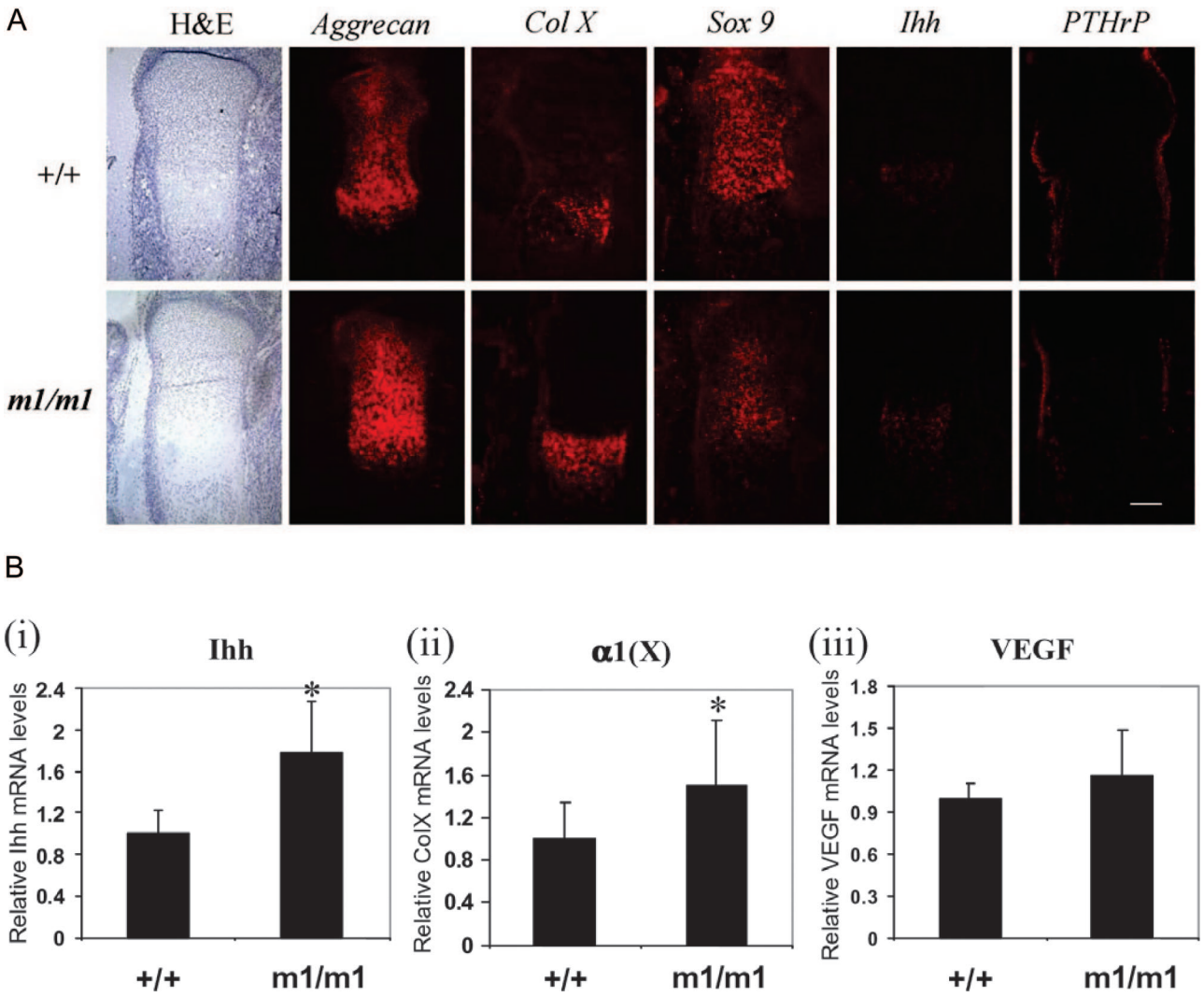

Figure 5. Analysis of chondrocyte differentiation in the embryonic growth plate of *Matn3* null mice. **A:** *In situ* hybridization of E16.5 proximal tibial epiphyseal growth plates from wild-type (+/+) and *Matn3* null (*m1/m1*) mice was performed using probes against *aggrecan*, *collagen type X* (*Col X*), *Sox9*, *Ihh*, and *PTHrP*. Scale bar = 600 μm. **B:** Real-time quantitative RT-PCR analysis of RNA isolated from E18.5 wild-type and *Matn3* null limbs shows that the mRNA levels of *Ihh* and *Col X* are significantly increased in *Matn3* null chondrocytes, whereas the level of *VEGF* mRNA remains unchanged. Statistical significance was taken at *P* values of less than 0.05 ($P < 0.05$).

whether the expanded hypertrophic zone seen in embryonic endochondral bone formation would have any effect on the mineral density of bones in the adult. Dual-energy X-ray absorptiometry densitometry was used to measure whole-body and knee joint BMD of *Matn3* null mice at various ages. As expected, both *Matn3* null and wild-type mice showed a gradual increase in whole-body BMD levels with age (Figure 6A); however, by 18 weeks of age *Matn3* null mice showed a significantly elevated BMD (0.062 ± 0.003) compared with both wild-type mice (0.054 ± 0.003) and *Matn1* null mice (0.054 ± 0.002) (Figure 6B). When the knee joints were analyzed separately, wild-type mice showed a relatively stable BMD value at different ages, whereas *Matn3* null mice showed elevated BMD values starting from 7 weeks of age (Figure 6C). The differences were most overt by 18 weeks of age (*Matn3* null, 0.093 ± 0.007; *Matn1* null, 0.077 ± 0.006; and wild-type, 0.073 ± 0.007) (Figure 6B). Therefore, adult *Matn3* null mice have significantly higher bone mass density than wild-type littermates or *Matn1* null mice.

Development of Osteoarthritis in Matrilin-3 Null Mice during Aging

Because elevated BMD is one feature of osteoarthritis, the articular cartilage of *Matn3* null mice knee joints were examined for evidence of osteoarthritis. Osteoarthritis of the knee joint cartilage in *Matn3* null mice was not observed in 7-week-old mice, occurred infrequently in 18 week mice (data not shown), but affected 100% of mice at 1 year of age (Table 1). In contrast, 45% of wild-type mice exhibited osteoarthritis at 1 year of age but of a less severe grade (Table 1). The histological features of osteoarthritis included fissuring of the articular surface, clustering of chondrocytes, formation of osteophytes, de-

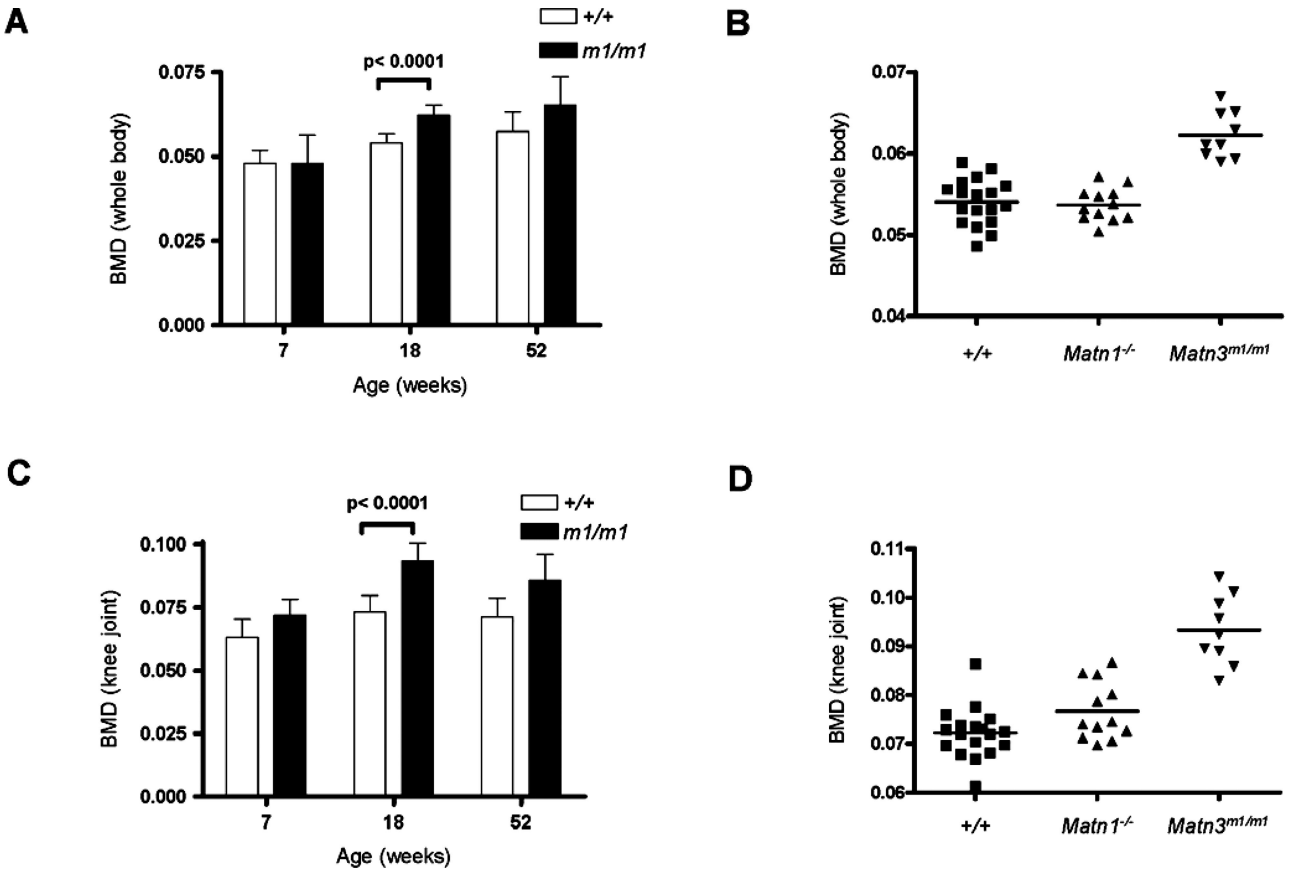

Figure 6. Measurement of BMD in adult *Matn3* null mice. Dual-energy X-ray absorptiometry densitometry was used to measure whole-body (**A**) and knee joint (**C**) BMD in wild-type and *Matn3* null (*m1/m1*) mice at different ages. **B** and **D:** Elevated BMD at 18 weeks of age was observed in *Matn3* null but not wild-type or *Matn1* null ($Matn1^{-/-}$) mice.

generation of the matrix, cleft of cartilage, and even exposure of the subchondral bone surface (Figure 7A). Staining of the *Matn3* null mice knee joint sections with Safranin-O/Fast Green indicated the loss of proteoglycan from articular cartilage and degradation of cartilage matrix (Figure 7B). Furthermore, the subchondral bone area was increased, which coincides with the decrease of bone marrow area (Figure 7B). Faxitron radiographical analysis of *Matn3* null mice showed characteristics of osteoarthritis including narrowing of joint space and increase of subchondral bone density (Figure 7C). Therefore, osteoarthritis occurs with higher incidence and more severity in adult matrilin-3 null mice during aging despite the lack of chondrodysplasia in postnatal development.

Discussion

At the onset of bone formation, mesenchymal cells of chondrogenic progeny undergo condensation followed by differentiation into chondrocytes. These chondrocytes then undergo a process of proliferation, maturation, and hypertrophy, followed by calcification of the ECM, cell death, and replacement by bone. In adults, articular cartilage remains at the surface of the bones, where it provides a smooth surface and confers weight-bearing strength to the joints. The ECM secreted by the chondrocytes provides the fundamental structure of cartilage and is rich in collagens (collagen types II, IX, and XI), proteoglycans (aggrecan), and other matrix proteins (cartilage

Table 1. Percentage of Different Grades of Osteoarthritic Knee Joints in Wild-Type and *Matn3* Null Mice at 52 Weeks

Group	Grade 0	Grade 1	Grade 2	Grade 3	Grade 4
+/+ (n = 9)	55.6	33.3	11.1	0.0	0.0
			*P = 0.001		
m1/m1 (n = 7)	0.0	28.6	14.3	28.6	28.6

*Comparison of healthy (grade 0) and OA cartilage morphological changes (pooled grades from 1 to 4; grade 1, slight fissuring and fibrillation of the superficial zone; grade 2, cleft and defect in the middle zone; grade 3, severe degeneration and deep cleft in the deep and calcification zones; and grade 4, exposure of the subchondral bone and bone erosion). Grades were determined by modified Wilhelmi OA scoring system with the single worst affected score of H&E paraffin slides through the entire knee joint. At least two blinded observers score the cartilage sections. Significance of scores between *Matn3* null (*m1/m1*) and wild-type (+/+) mice was determined by χ^2 statistics.

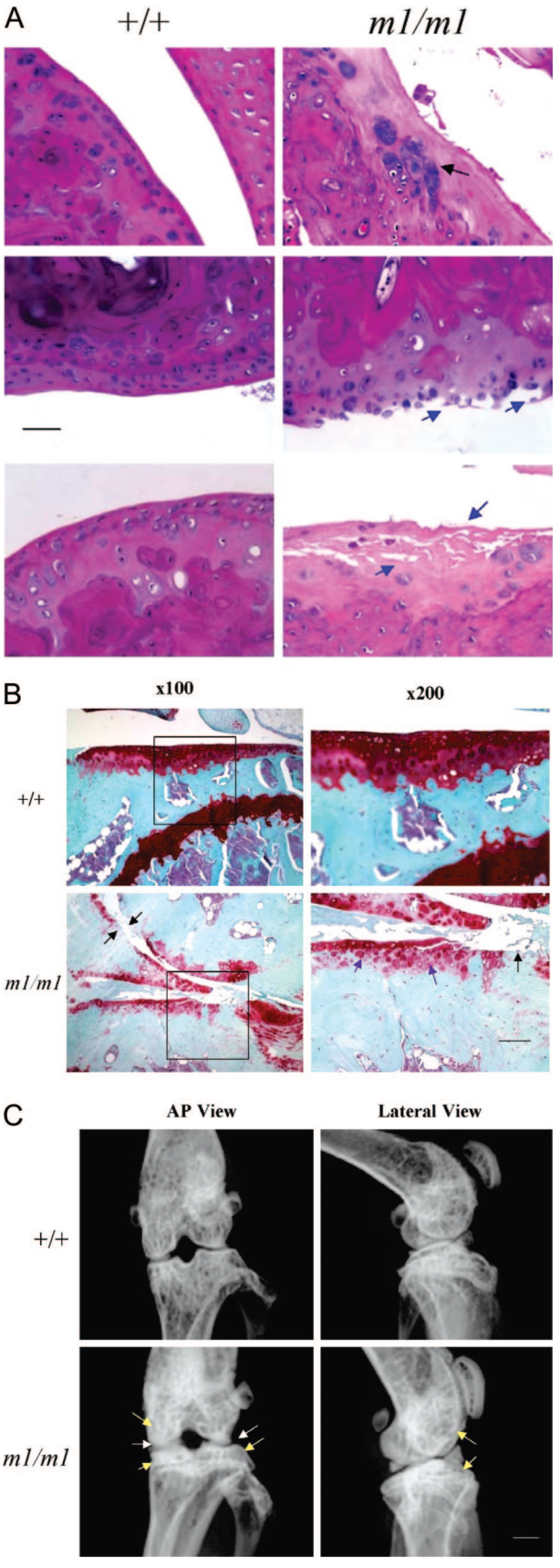

oligomeric matrix protein and matrilins).[33] Defects in cartilage formation and maintenance can lead to phenotypes ranging from relatively rare osteochondrodysplasias to the common degeneration of articular cartilage resulting in osteoarthritis.[34]

All four members of the matrilin family of proteins are expressed in developing cartilage and play an important role in the ECM through the formation of self-assembled filamentous networks[35–37]. To date, matrilin-3 is the only member of this family found to be associated with osteochondrodysplasias. In humans, mutations in the matrilin-3 gene (*MATN3*) have been found in patients with MED, bilateral hereditary microepiphyseal dysplasia, spondylo-epi-metaphyseal dysplasia, and idiopathic hand osteoarthritis,[13–19] and up-regulation of matrilin-3 has been found in a cohort of Swedish osteoarthritic patients.[20] OA is often associated with the increase of extracellular matrix molecules, although the lack of such functional ECM molecules often leads to OA as well.[20] This may be an attempt of the repairing process by OA chondrocytes.

To more fully understand the role of matrilin-3, we ablated the matrilin-3 gene (*Matn3*). *Matn3* null mice were viable and fertile and had a normal lifespan. Adult *Matn3* null mice revealed no gross skeletal malformation, and the architecture of the epiphyseal proximal growth plate of tibiae from newborn *Matn3* null mice (P1) showed no difference from wild-type littermates, similar to a previous report.[25] However, in contrast to the suggestion of functional redundancy between the matrilins,[25] we found that the embryonic epiphyseal proximal growth plates from *Matn3* null mice tibiae clearly showed an expansion of the hypertrophic zone of chondrocytes (most prominent at E16.5).

A number of secreted polypeptides and transcription factors are known to cooperatively regulate the rates of proliferation of chondrocytes and their transition to hypertrophy. Parathyroid hormone-related peptide (PTHrP), together with Ihh, controls the rate of chondrocyte proliferation and the transition of these cells to hypertrophy.[38] PTHrP signals through activating protein kinase A and has been postulated to negatively regulate chondrocyte maturation by increasing the activity of Sox9,[39] a transcription factor that inhibits chondrocyte hypertrophy.[38,40] Another important factor is vascular endothelial growth factor (VEGF), which is expressed by hypertrophic chondrocytes and an essential coordinator of chondrocyte death, chondroclast function, extracellular matrix remodeling, angiogenesis, and bone formation in the

Figure 7. Analysis of onset osteoarthritis (OA) in adult *Matn3* null mice. Analysis of sections from the knee joint of 52-week-old wild-type and *Matn3* null (*m1/m1*) mice by H&E staining (**A**, **black arrows** show clustering of chondrocytes and osteophyte formation, and **blue arrows** show fibrillation and degradation of the articular cartilage surface; scale bar = 500 μm) and Safranin-O staining (**B**, **purple arrows** show the decrease of proteoglycan staining in articular cartilage, and **black arrows** show the loss of cartilage and the exposure of the subchondral bone plate; **boxed area** on ×100 images are the enlarged in the ×200 images; scale bar = 500 μm). **C:** Faxitron radiographical analysis of the knee joints from 52-week-old wild-type and *Matn3* null mice, with **white arrows** indicating the narrowing of the joint space and **yellow arrows** indicating the increase of subchondral bone density (scale bar = 1 mm).

growth plate.[41] Transcripts for *Sox9* and *Pthrp* but not *VEGF* were present at lower levels in the embryonic growth plates of *Matn3* null mice than the wild-type controls, indicating that the expanded hypertrophic zone is due to accelerated differentiation of the chondrocytes rather than delayed matrix resorption.

Our data indicate that the accelerated differentiation of *Matn3* null chondrocytes may result from precocious entry to the prehypertrophic stage from the proliferation stage. A premature exit from the cell cycle is suggested by a significant decrease of proliferating chondrocytes in the columnar region of the *Matn3* null proximal tibial growth plate compared with the wild-type. A precocious entry into the prehypertrophic stage is suggested by the up-regulation of *Ihh* mRNA in the *Matn3* null tibial growth plate. Down-regulation of Sox9 in *Matn3* null tibial growth plates may cause premature prehypertrophy, because Sox family proteins have been shown to keep chondrocytes proliferating, to delay prehypertrophy, and to down-regulate Ihh signaling.[42] Although the reduced levels of *Sox9* is most likely responsible for the accelerated transition of the chondrocytes to hypertrophy, it is unclear how loss of matrilin-3 expression would induce this. This is the first report of a member of the matrilin family regulating *Sox9* expression, either directly or indirectly. Alterations of cartilage matrix may primarily affect the diffusion and sequestration of extracellular growth/differentiation factors including Ihh, PthrP, FGFs, BMPs, and Wnts and secondarily chondrocyte differentiation and hence the expression of these regulatory genes. It remains to be determined whether matrilin-3 interacts with these factors or their binding proteins.

Expanded zones of hypertrophic chondrocytes in the epiphyseal growth plate have been observed in several other knockout mice, including those deficient in Smad3,[43] Fgfr3,[44,45] Fgf18,[46] and connective tissue growth factor.[47] However, the significance of this in the *Matn3* null mice is unclear because the expansion is only seen during embryonic stages, with the postnatal size of the hypertrophic zone being comparable with that seen in wild-type mice. *Matn3* null mice generated by Ko et al[25] also showed no histological abnormalities in endochondral bone formation in the adult (histological analysis of embryonic stages was not reported). Matrilin-3 has been shown to be expressed in the developing long bones after birth,[22] so the lack of an expanded hypertrophic zone in newborn and adult *Matn3* null mice cannot be explained by the reason that matrilin-3 is not normally present in the adult. Because the loss of matrilin-3 causes increased hypertrophic differentiation of growth plate chondrocytes in the embryo but not peri- or postnatally, we suggest that matrilin-3 is involved in modulating chondrocyte differentiation in an epiphyseal growth plate during the prenatal period only.

Our study reveals an unexpected property of matrilin-3 in maintaining proper BMD, a factor that was not previously examined.[25] BMD is regulated by both environmental and genetic factors (reviewed in Ref. [48]). Compared with wild-type mice, *Matn3* null mice showed significantly elevated whole-body and knee joint BMD values at 18 weeks of age, the time when mice typically reach peak bone density.[49] Increased BMD levels have also been reported in Smad1C transgenic mice,[50] GDF8 (myostatin)-deficient mice,[51] and Stat1-deficient mice.[52] It is tempting to speculate that the elevated BMD levels seen in *Matn3* null mice are due to an increase in mineralization of the ECM caused by increased Ihh expression and/or by decreased PTHrP distribution in perichondrium. Ihh is a potent stimulator of osteoblast differentiation and mineralization,[38,40] whereas PTHrP is an inhibitor of chondrocyte hypertrophy and mineralization. PTH/PTHrP-treated cultured hypertrophic chondrocytes show a repression of collagen type X expression, and the cells mimic proliferating cartilage and are unable to express alkaline phosphatase and mineralize.[53]

We also show for the first time that the loss of *Matn3* leads to onset of osteoarthritis (OA) with higher incidence and more severity in the mouse knee, which exhibit some features mimicking human osteoarthritis, including osteophyte formation, loss of proteoglycan from cartilage, articular cartilage degeneration, and increase of subchondral bone density. The absence of matrilin-3 in the pericellular matrix where it normally interacts with collagen and aggrecan could affect the biomechanical integrity of the cartilage matrix. In addition, clinical studies have shown that the prevalence of radiographical knee and hip osteoarthritis, especially in terms of osteophytes, increases with increasing BMD.[8,54–58] However, the mechanism of the association between increased bone density and joint degeneration is not known. Our data show that matrilin-3 deficiency results in both the increase of BMD and joint cartilage degeneration, thereby connecting these two events together. It is intriguing that the loss of a single molecule matrilin-3 would lead to these two processes, one occurring in the bone and the other occurring in articular cartilage. It is not known yet whether the changes in the subchondral bone cause cartilage degeneration, or vice versa, because matrilin-3 is expressed by both chondrocytes and osteoblasts.[59] However, the generation of the *Matn3* null mice provides a powerful animal model to study the relationship between articular cartilage and subchondral bone.

Our *Matn3* null mouse model is particularly relevant to studying pathogenesis of osteoarthritis given that MED patients suffer early-onset OA[14] and that mutations in *MATN3* have been reported in patients with idiopathic hand OA.[19] Macrostructural changes of the joints in MED patients resulting from chondrodysplasia during development may make them more susceptible to developing osteoarthritis. However, it is puzzling why *Matn3*-associated MED patients develop both chondrodysplasia and osteoarthritis, whereas *Matn3*-associated idiopathic hand OA patients do not have chondrodysplasia. Our data suggest that chondrodysplasia and osteoarthritis are not necessarily coupled in Matn3-defective cartilage because *Matn3* null mice develop higher incidence of osteoarthritis in adulthood without chondrodysplasia in childhood. The fact that the loss of matrilin-3 does not lead to postnatal chondrodysplasia suggests that this developmental disease is caused by a dominant-negative effect of the mutant matrilin-3, rather than by the lack of *Matn3*. On the other hand, the lack of the functional

Matn3 can at least partially account for the pathogenesis of OA associated with *Matn3* mutations.

Acknowledgments

We thank Evelyn Grau for microinjection of the targeted ES cell lines, the personnel of Team 83 (WTSI) for care and monitoring of the animals, and Veronique Lefebvre for discussion of data.

References

1. Deak F, Wagener R, Kiss I, Paulsson M: The matrilins: a novel family of oligomeric extracellular matrix proteins. Matrix Biol 1999, 18:55–64
2. Paulsson M, Heinegård D: Radioimmunoassay of the 148-kilodalton cartilage protein: distribution of the protein among bovine tissues. Biochem J 1982, 207:207–213
3. Wagener R, Kobbe B, Paulsson M: Primary structure of matrilin-3, a new member of a family of extracellular matrix proteins related to cartilage matrix protein (matrilin-1) and von Willebrand factor. FEBS Lett 1997, 413:129–134
4. Klatt AR, Nitsche DP, Kobbe B, Morgelin M, Paulsson M, Wagener R: Molecular structure and tissue distribution of matrilin-3, a filament-forming extracellular matrix protein expressed during skeletal development. J Biol Chem 2000, 275:3999–4006
5. Piecha D, Muratoglu S, Morgelin M, Hauser N, Studer D, Kiss I, Paulsson M, Deak F: Matrilin-2, a large, oligomeric matrix protein, is expressed by a great variety of cells and forms fibrillar networks. J Biol Chem 1999, 274:13353–13361
6. Klatt A, Nitsche DP, Kobbe B, Macht M, Paulsson M, Wagener R: Molecular structure, processing, and tissue distribution of matrilin-4. J Biol Chem 2001, 276:17267–17275
7. Wu JJ, Eyre DR: Matrilin-3 forms disulfide-linked oligomers with matrilin-1 in bovine epiphyseal cartilage. J Biol Chem 1998, 273:17433–17438
8. Zhang Y, Chen Q: Changes of matrilin forms during endochondral ossification: molecular basis of oligomeric assembly. J Biol Chem 2000, 275:32628–32634
9. Winterbottom N, Tondravi MM, Harrington TL, Klier FG, Vertel BM, Goetinck PF: Cartilage matrix protein is a component of the collagen fibril of cartilage. Dev Dyn 1992, 193:266–276
10. Paulsson M, Heinegård D: Matrix proteins bound to associatively prepared proteoglycans from bovine cartilage. Biochem J 1979, 183:539–545
11. Hauser N, Paulsson M, Heinegård D, Morgelin M: Interaction of cartilage matrix protein with aggrecan: increased covalent cross-linking with tissue maturation. J Biol Chem 1996, 271:32247–32252
12. Wiberg C, Klatt AR, Wagener R, Paulsson M, Bateman JF, Heinegård D, Mörgelin M: Complexes of matrilin-1 and biglycan or decorin connect collagen VI microfibrils to both collagen II and aggrecan. J Biol Chem 2003, 278:37698–37704
13. Jackson GC, Barker FS, Jakkula E, Czarny-Ratajczak M, Makitie O, Cole WG, Wright MJ, Smithson SF, Suri M, Rogala P, Mortier GR, Baldock C, Wallace A, Elles R, Ala-Kokko L, Briggs MD: Missense mutations in the beta strands of the single A-domain of matrilin-3 result in multiple epiphyseal dysplasia. J Med Genet 2004, 41:52–59
14. Chapman KL, Mortier GR, Chapman K, Loughlin J, Grant ME, Briggs MD: Mutations in the region encoding the von Willebrand factor A domain of matrilin-3 are associated with multiple epiphyseal dysplasia. Nat Genet 2001, 28:393–396
15. Mostert AK, Dijkstra PF, Jansen BR, van Horn JR, de Graaf B, Heutink P, Lindhout D: Familial multiple epiphyseal dysplasia due to a matrilin-3 mutation: further delineation of the phenotype including 40 years follow-up. Am J Med Genet 2003, 120A:490–497
16. Makitie O, Mortier GR, Czarny-Ratajczak M, Wright MJ, Suri M, Rogala P, Freund M, Jackson GC, Jakkula E, Ala-Kokko L, Briggs MD, Cole WG: Clinical and radiographic findings in multiple epiphyseal dysplasia caused by MATN3 mutations: description of 12 patients. Am J Med Genet 2004, 125A:278–284
17. Mabuchi A, Haga N, Maeda K, Nakashima E, Manabe N, Hiraoka H, Kitoh H, Kosaki R, Nishimura G, Ohashi H, Ikegawa S: Novel and recurrent mutations clustered in the von Willebrand factor A domain of MATN3 in multiple epiphyseal dysplasia. Hum Mutat 2004, 4:439–440
18. Borochowitz ZU, Scheffer D, Adir V, Dagoneau N, Munnich A, Cormier-Daire V: Spondylo-epi-metaphyseal dysplasia (SEMD) matrilin 3 type: homozygote matrilin 3 mutation in a novel form of SEMD. J Med Genet 2004, 41:366–372
19. Stefansson SE, Jonsson H, Ingvarsson T, Manolescu I, Jonsson HH, Olafsdottir G, Palsdottir E, Stefansdottir G, Sveinbjornsdottir G, Frigge ML, Kong A, Gulcher JR, Stefansson K: Genomewide scan for hand osteoarthritis: a novel mutation in matrilin-3. Am J Hum Genet 2003, 72:1448–1459
20. Pullig O, Weseloh G, Klatt AR, Wagener R, Swoboda B: Matrilin-3 in human articular cartilage: increased expression in osteoarthritis. Osteoarthritis Cartilage 2002, 10:253–263
21. Segat D, Frie C, Nitsche PD, Klatt AR, Piecha D, Korpos E, Deak F, Wagener R, Paulsson M, Smyth N: Expression of matrilin-1, -2 and -3 in developing mouse limbs and heart. Matrix Biol 2000, 19:649–655
22. Klatt AR, Paulsson M, Wagener R: Expression of matrilins during maturation of mouse skeletal tissues. Matrix Biol 2002, 21:289–296
23. Aszodi A, Bateman JF, Hirsch E, Baranyi M, Hunziker EB, Hauser N, Bosze Z, Fassler R: Normal skeletal development of mice lacking matrilin 1: redundant function of matrilins in cartilage? Mol Cell Biol 1999, 19:7841–7845
24. Huang X, Birk DE, Goetinck PF: Mice lacking matrilin-1 (cartilage matrix protein) have alterations in type II collagen fibrillogenesis and fibril organization. Dev Dyn 1999, 216:434–441
25. Ko Y, Kobbe B, Nicolae C, Miosge N, Paulsson M, Wagener R, Aszodi A: Matrilin-3 is dispensable for mouse skeletal growth and development. Mol Cell Biol 2004, 24:1691–1699
26. Ramirez-Solis R, Liu P, Bradley A: Chromosome engineering in mice. Nature 1995, 378:720–724
27. McMahon AP, Bradley A: The Wnt-1 (int-1) proto-oncogene is required for development of a large region of the mouse brain. Cell 1990, 62:1073–1085
28. Lufkin T, Mark M, Hart CP, Dolle P, LeMeur M, Chambon P: Homeotic transformation of the occipital bones of the skull by ectopic expression of a homeobox gene. Nature 1992, 359:835–841
29. Wilhelmi G, Faust R: Suitability of the C57 black mouse as an experimental animal for the study of skeletal changes due to ageing, with special reference to osteo-arthrosis and its response to tribenoside. Pharmacology 1976, 14:289–296
30. Chen Q, Johnson DM, Haudenschild DR, Tondravi MM, Goetinck PF: Cartilage matrix protein forms a type II collagen-independent filamentous network: analysis in primary cell cultures with a retrovirus expression system. Mol Biol Cell 1996, 6:1743–1753
31. Lee JO, Rieu P, Arnaout MA, Liddington R: Crystal structure of the A domain from the alpha subunit of integrin CR3 (CD11b/CD18). Cell 1995, 80:631–638
32. Birk DE, Trelstad RL: Extracellular compartments in tendon morphogenesis: collagen fibril, bundle, and macroaggregate formation. J Cell Biol 1986, 103:231–240
33. Morris NP, Keene DR, Horton WA: Cartilage morphology. Extracellular Matrix and Heritable Disorders of Connective Tissue, ed 2. Edited by PM Rocye, B Steinmann. New York, Alan R. Liss, 2002
34. Chapman KL, Briggs MD, Mortier GR: Review: clinical variability and genetic heterogeneity in multiple epiphyseal dysplasia. Pediatr Pathol Mol Med 2003, 22:53–75
35. Chen Q, Zhang Y, Johnson DM, Goetinck PF: Assembly of a novel cartilage matrix protein filamentous network: molecular basis of differential requirement of von Willebrand factor A domains. Mol Biol Cell 1999, 10:2149–2162
36. Makihira S, Yan W, Ohno S, Kawamoto T, Fujimoto K, Okimura A, Yoshida E, Noshiro M, Hamada T, Kato Y: Enhancement of cell adhesion and spreading by a cartilage-specific noncollagenous protein, cartilage matrix protein (CMP/Matrilin-1), via integrin alpha1beta1. J Biol Chem 1999, 274:11417–11423
37. Whittaker CA, Hynes RO: Distribution and evolution of von Willebrand/integrin A domains: widely dispersed domains with roles in cell adhesion and elsewhere. Mol Biol Cell 2002, 13:3369–3387
38. Vortkamp A, Lee K, Lanske B, Segre GV, Kronenberg HM, Tabin CJ: Regulation of rate of cartilage differentiation by Indian hedgehog and PTH-related protein. Science 1996, 273:613–622

39. Huang W, Chung UI, Kronenberg HM, de Crombrugghe B: The chondrogenic transcription factor Sox9 is a target of signaling by the parathyroid hormone-related peptide in the growth plate of endochondral bones. Proc Natl Acad Sci USA 2001, 98:160–165
40. Lanske B, Karaplis AC, Lee K, Luz A, Vortkamp A, Pirro A, Karperien M, Defize LH, Ho C, Mulligan RC, Abou-Samra AB, Juppner H, Segre GV, Kronenberg HM: PTH/PTHrP receptor in early development and Indian hedgehog-regulated bone growth. Science 1996, 273:663–666
41. Gerber HP, Vu TH, Ryan AM, Kolwalski J, Werb Z, Ferrara N: VEGF couples hypertrophic cartilage remodelling, ossification and angiogenesis during endochondral bone formation. Nat Med 1999, 5:623–628
42. Smits P, Dy P, Mitra S, Lefebvre V: Sox5 and Sox6 are needed to develop and maintain source, columnar, and hypertrophic chondrocytes in the cartilage growth plate. J Cell Biol 2004, 164:747–758
43 Yang X, Chen L, Xu X, Li C, Huang C, Deng CX: TGF-beta/Smad3 signals repress chondrocyte hypertrophic differentiation and are required for maintaining articular cartilage. J Cell Biol 2001, 153:35–46
44. Naski MC, Colvin JS, Coffin JD, Ornitz DM: Repression of hedgehog signaling and BMP4 expression in growth plate cartilage by fibroblast growth factor receptor 3. Development 1998, 125:4977–4988
45. Ornitz DM: Regulation of chondrocyte growth and differentiation by fibroblast growth factor receptor 3. Novartis Found Symp 2001, 232:63–76
46. Liu Z, Xu J, Colvin JS, Ornitz DM: Coordination of chondrogenesis and osteogenesis by fibroblast growth factor 18. Genes Dev 2002, 16:859–869
47. Ivkovic S, Yoon BS, Popoff SN, Safadi FF, Libuda DE, Stephenson RC, Daluiski A, Lyons KM: Connective tissue growth factor coordinates chondrogenesis and angiogenesis during skeletal development. Development 2003, 130:2779–2791
48. Brandi ML, Gennari L, Cerinic MM, Becherini L, Falchetti A, Masi L, Gennari C, Reginster JY: Genetic markers of osteoarticular disorders: facts and hopes. Arthritis Res 2001, 3:270–280
49. Beamer WG, Donahue LR, Rosen CJ, Baylink DJ: Genetic variability in adult bone density among inbred strains of mice. Bone 1996, 18:397–403
50. Liu Z, Shi W, Ji X, Sun C, Jee WSS, Wu Y, Mao Z, Nagy TR, Li Q, Cao X: Molecules mimicking Smad1 interacting with Hox stimulate bone formation. J Biol Chem 2004, 279:11313–11319
51. Hamrick MW: Increased bone mineral density in the femora of GDF8 knockout mice. Anat Rec A Discov Mol Cell Evol Biol 2003, 272:388–391
52. Xiao L, Naganawa T, Obugunde E, Gronowicz G, Ornitz DM, Coffin JD, Hurley MM: Stat1 controls postnatal bone formation by regulating fibroblast growth factor signaling in osteoblasts. J Biol Chem 2004, 279:27743–27752
53. Zerega B, Cermelli S, Bianco P, Cancedda R, Cancedda FD: Parathyroid hormone [PTH(1–34)] and parathyroid hormone-related protein [PTHrP(1–34)] promote reversion of hypertrophic chondrocytes to a prehypertrophic proliferating phenotype and prevent terminal differentiation of osteoblast-like cells. J Bone Miner Res 1999, 14:1281–1289
54. Hannan MT, Anderson JJ, Zhang Y, Levy D, Felson DT: Bone mineral density and knee osteoarthritis in elderly men and women: the Framingham Study. Arthritis Rheum 1993, 36:1671–1680
55. Hart DJ, Mootoosamy I, Doyle DV, Spector TD: The relationship between osteoarthritis and osteoporosis in the general population: the Chingford Study. Ann Rheum Dis 1994, 53:158–162
56. Nevitt MC, Lane NE, Scott JC, Hochberg MC, Pressman AR, Genant HK, Cummings SR: Radiographic osteoarthritis of the hip and bone mineral density: the Study of Osteoporotic Fractures Research Group. Arthritis Rheum 1995, 38:907–916
57. Burger H, van Daele PL, Odding E, Valkenburg HA, Hofman A, Grobbee DE, Schutte HE, Birkenhager JC, Pols HA: Association of radiographically evident osteoarthritis with higher bone mineral density and increased bone loss with age: the Rotterdam Study. Arthritis Rheum 1996, 39:81–86
58. Sowers M, Lachance L, Jamadar D, Hochberg MC, Hollis B, Crutchfield M, Jannausch ML: The associations of bone mineral density and bone turnover markers with osteoarthritis of the hand and knee in pre- and perimenopausal women. Arthritis Rheum 1999, 42:483–489
59. Korpos E, Molnar A, Papp P, Kiss I, Orosz L, Deak F: Expression pattern of matrilins and other extracellular matrix proteins characterize distinct stages of cell differentiation during antler development. Matrix Biol 2005, 24:124–135